Influence of Iron-Removal Procedures on Sequential Electron Transfer in Photosynthetic Bacterial Reaction Centers Studied by Transient EPR Spectroscopy†

Lisa M. Utschig, Scott R. Greenfield, Jau Tang, Philip D. Laible, and Marion C. Thurnauer*

Chemistry Division, Argonne National Laboratory, Argonne, Illinois 60439

Received December 10, 1996; Revised Manuscript Received May 5, 1997⊗

ABSTRACT: Electron spin polarized electron paramagentic resonance (ESP EPR) spectra were obtained with deuterated iron-removed photosynthetic bacterial reaction centers (RCs) to specifically investigate the effect of the rate of primary charge separation, metal-site occupancy, and H-subunit content on the observed $P_{865}{}^{+}Q_A{}^{-}$ charge-separated state. Fe-removed and Zn-substituted RCs from *Rb. sphaeroides* R-26 were prepared by refined procedures, and specific electron transfer rates (k_Q) from the intermediate acceptor H^- to the primary acceptor Q_A of $(200\ ps)^{-1}$ vs $(3-6\ ns)^{-1}$ were observed. Correlation of the transient EPR and optical results shows that the observed slow k_Q rate in Fe-removed RCs is H-subunit-independent, and, in some cases, independent of Fe-site occupancy as Zn^{2+} substitution does not ensure retention of the native k_Q. In addition, shifts in the optical spectrum of P_{865} and differences in the high-field region of the Q-band ESP spectrum for Fe-removed RCs with slow k_Q indicate possible structural changes near P_{865}. The experimental X-band and Q-band spin-polarized EPR spectra for deuterated Fe-removed RCs where k_Q is at least 15-fold slower at room temperature than the $(200\ ps)^{-1}$ rate observed for native Fe-containing RCs have different relative amplitudes and small *g*-value shifts compared to the spectra of Zn-RCs which have a k_Q unchanged from native RCs. These differences reflect the trends in polarization predicted from the sequential electron transfer polarization (SETP) model [Morris et al. (1995) *J. Phys. Chem. 99,* 3854−3866; Tang et al. (1996) *Chem. Phys. Lett. 253,* 293−298]. Thus, SETP modeling of these highly resolved ESP spectra obtained with well-characterized proteins will provide definitive information about any light-induced structural changes of P_{865}, H, and Q_A that occur upon formation of the $P_{865}{}^{+}Q_A{}^{-}$ charge-separated state.

The key reaction of photosynthetic conversion of light into useful chemical energy involves rapid, sequential electron transfer resulting in charge separation. The prime example of this process is the sequential electron transfer that takes place in the purple photosynthetic bacterial reaction center (RC). High-resolution crystal structures (Allen et al., 1988; El-Kabbani et al., 1991; Ermler et al., 1994) show that the bacterial RC consists of three 30−35 kDa protein subunits, the two transmembrane pigment-containing subunits L and M and the cytoplasmic hydrophilic H-subunit. Intricately anchored within the protein matrix are one high-spin iron-(II) and eight chromophores, including four bacteriochlorophylls (Bchls), two bacteriopheophytins (Bphs), and two quinones (Q). Efficient photoinitiated charge separation occurs sequentially; (i) ∼3 ps after photoexcitation of a special pair of Bchls (P), the primary radical pair P^+H^- is formed, where H denotes a monomeric Bph, followed by (ii) an electron transfer step in which the electron is transferred from H^- to the primary quinone electron acceptor Q_A within 200 ps to create the membrane-spanning secondary electron pair $P^+Q_A{}^-$. Within 200 μs, the electron reaches the secondary electron acceptor Q_B.

In order to obtain a complete understanding of photosynthetic electron transfer, the relationship of electron transfer kinetics to dynamic protein structure must be elucidated. One structure−function relationship that has not clearly been defined is the role of the non-heme iron. In the bacterium *Rhodopseudomonas sphaeroides* R-26, the two ubiquinone electron acceptors, Q_A and Q_B, are magnetically coupled to the Fe^{2+} [for reviews, see Feher and Okamura (1978, 1984) and Wraight (1982)]. The Fe^{2+} apparently does not facilitate electron transfer between Q_A and Q_B, and substitution of different divalent metal ions into the Fe site does not significantly alter the electron transfer characteristics (Debus et al., 1986). Although not required for primary photochemical activity, removal of the non-heme Fe^{2+} from the RC protein dramatically influences the electron transfer rate (k_Q) from the reduced pheophytin intermediate H^- to the first quinone acceptor Q_A (Kirmaier et al., 1986). If the Fe^{2+} is removed to form the apoprotein and all three protein subunits remain intact, a 20-fold reduction in this electron transfer rate relative to the rate observed in native Fe-containing RCs is observed (Kirmaier et al., 1986, Liu et al., 1991). When either the native Fe^{2+} is replaced with Zn^{2+} or both the H-subunit and the Fe^{2+} are removed, k_Q is unchanged from that observed for native RCs (Blankenship & Parson, 1979; Kirmaier et al., 1986; Liu et al., 1991). One possible explanation for this dramatic change in rate is the "spring-model", where the position of Q_A is influenced by both the

† This work was supported by the U.S. Department of Energy, Office of Basic Energy Sciences, Division of Chemical Sciences, under Contract W-31-109-Eng-38.

* Correspondence should be addressed to this author at the Chemistry Division D-200, Argonne National Laboratory, 9700 S. Cass Ave., Argonne, IL 60439. Phone: (630) 252-3570. Fax: (630) 252-9289. Email: THURNAUER@ANLCHM.CHM.ANL.GOV.

⊗ Abstract published in *Advance ACS Abstracts,* July 1, 1997.

S0006-2960(96)03031-0 CCC: $14.00 © 1997 American Chemical Society

Fe^{2+} and the H-subunit (Liu et al., 1991; Schelvis et al., 1992). Other possibilities include a localized change in the quinone binding pocket, such as H-bonding (van der Est et al., 1995), that affects the redox properties of Q_A upon Fe removal. Fe removal might even induce structural changes at a distance by altering the relative orientations of Bph or special pair P_{865}. Other experiments have shown, however, that large changes in $P_{865}{}^{+}Q_A{}^{-}$ recombination or Q_A to Q_B electron transfer rates can occur without large changes in the donor/acceptor geometries (Franzen et al., 1990; van den Brink et al., 1994; Tiede et al., 1996). These results implicate a role for protein reorganization energy in controlling electron transfer processes. Fe removal might have similar effects on global protein dynamics.

One method to sort out what parameters are dominant in determining significant changes in electron transfer rates is to examine the transient electron paramagnetic resonance (EPR) spectra of the light-induced electron spin polarized (ESP) radical pair state $P_{865}{}^{+}Q_A{}^{-}$ (van den Brink et al., 1994; Bittl et al., 1996). ESP signals are sensitive to the geometry of this state and can also provide structural details of the intermediate transient $P_{865}{}^{+}H^{-}$ radical pair (Morris et al., 1995). We have used these techniques to investigate the influence of the H-subunit and Fe^{2+} on the cofactor orientation and electron transfer processes in the RC from *Rb. sphaeroides* R-26. In order to obtain reliable results with these EPR methods, one must have well-characterized RC samples with respect to the metal-site occupancy and kinetics of electron transfer. Therefore, we have refined the preparation procedures for Fe removal and Zn substitution of RCs. Analytical and spectroscopic characterization of these Fe-removed RCs provides new insights into the Fe-removal procedures. These modified procedures consistently produce samples that have the native "fast" $(200\ ps)^{-1}$ or "slow" $(3-6\ ns)^{-1}$ k_Q rates.

Transient EPR spectra of the radical pair state $P^{+}{}_{865}Q_A{}^{-}$ in fully deuterated RCs with k_Q determined to be "fast" or "slow" were obtained. Deuteration reduces the inhomogeneous line width of the EPR signal due to unresolved hyperfine interactions providing improved resolution at X-band and Q-band, and thus increased sensitivity to orientation parameters of the cofactors. The sequential electron transfer polarization (SETP) model (Norris et al., 1990; Morris et al., 1995; Tang et al., 1996; Hore, 1996), in which the singlet−triplet mixing developed in the intermediate radical pair is projected onto the correlated radical pair polarization (CRPP) developed on the final radical pair, can be used to interpret the observed signals. Characterization of the ESP EPR signals provides both kinetic and structural details of the charge separation process, including information about the transient species that precedes the stabilized charge-separated state (Snyder & Thurnauer, 1993). Other laboratories have attempted to obtain structural information of the charge-separated state in the bacterial reaction center, but have thus far neglected the sequential nature of electron transfer in their data simulations (Füchsle et al., 1993; van der Est et al., 1993; Prisner et al., 1995). In this paper, we report highly resolved X-band and Q-band ESP EPR spectra of deuterated Fe-removed RCs where the k_Q electron transfer rate has been altered and interpret these results in terms of how the metal ion and subunit compositions influence protein function. Our results address the importance of including the sequential nature of the electron transfer process to describe the observed ESP signal. Transient optical and EPR results show that the observed reductions in the k_Q electron transfer rate are H-subunit-independent. ESP EPR spectra of these biochemically altered proteins potentially could provide insight about the importance of donor/acceptor geometries versus protein reorganization energies in regulating electron transfer processes in photosynthetic proteins.

EXPERIMENTAL PROCEDURES

Preparation of the Reaction Centers. Reaction centers from the photosynthetic bacterium *Rb. sphaeroides* R-26 were isolated according to the procedure of Wraight (1979) adapted by Tiede (Tiede et al., 1996). Deuterated reaction centers were isolated from whole cells of *Rb. sphaeroides* R-26 which were grown in D_2O (99.7%) on deuterated substrates (Crespi, 1982). Deuterated ubiquinone-10 was obtained from these cells using the method of Hale et al. (1983). The amount and type of detergent used in the RC isolation were critical to the success of the Fe-removal procedure and H-subunit retention; the purification (Tiede et al., 1996) was modified accordingly. The final 0.25 g/mL $(NH_4)_2SO_4$ floatate was dissolved in 0.15% lauryldimethylamine *N*-oxide (LDAO), 10 mM Tris-HCl at pH 7.9, 10 μM EDTA, and 100 mM NaCl. The protein was loaded onto a sucrose gradient (20−40% w/v) with 10 mM Tris-HCl at pH 7.9 and 0.04% LDAO and centrifuged overnight at 50 000 rpm. The reaction center band was collected and dialyzed against 10 mM Tris-HCl, 10 μM EDTA at pH 7.9, and 0.045% LDAO. The protein was loaded onto a DEAE-Sephacel column and washed with 0.045% LDAO, 60 mM NaCl, 10 μM EDTA, and 10 mM Tris-HCl at pH 8.0 and eluted by increasing the NaCl concentration of the buffer to 280 mM. The protein was eluted such that several 0.5−1 mL concentrated ($OD_{800} \sim 18-20\ cm^{-1}$) fractions were collected. These fractions were cryogenically frozen in liquid N_2 and stored at −80 °C. The final 280 nm/802 nm ratios were 1.2 to 1.3. RC concentration was determined with the extinction coefficient $\epsilon_{802} = 288\ mM^{-1}\ cm^{-1}$ (Straley et al., 1973).

Fe Removal with Zn Replacement (Zn-RCs). Deuterated RCs (∼0.5−1.0 mL; $OD_{803} = 19-20\ cm^{-1}$ in 10 mM Tris-HCl, pH 7.9, 10 μM EDTA, 280 mM NaCl, and 0.045% LDAO) were incubated 5 min at 25 °C in 5 mM *o*-phenanthroline, 20 mM Tris-HCl, and 3 equiv of deuterated ubiquinone-10. The stock solutions were 135 mM *o*-phenanthroline (30% ethanol) and a 1 M solution of Tris-HCl, pH 8.0. Ubiquinone-10 was added from a 2 mM stock solution prepared by suspending the quinone in 1% LDAO and heating to 65 °C. 1.5 M LiSCN was added to the RC solution from a 3.9 M LiSCN stock solution (concentration determined by ICP-AES) followed by ice temperature incubation. After 30 min, 8 mM 2-mercaptoethanol and 1 mM $ZnSO_4$ were added, and the protein was again incubated on ice. After 30 min, the protein was transferred to 10 mm wide 12 000−14 000 MWCO dialysis tubing (Spectra/Por) and dialyzed 12 h at 4 °C versus 10 mM Tris-HCl, pH 7.9, 0.01 mM EDTA, 0.045% LDAO, and 5 g of Chelex 100 resin (Bio-Rad). Precipitated Zn and Fe thiocyanate complexes (white or light pink precipitate) were spun down, and the protein was frozen in liquid N_2 and stored at −80 °C until used for kinetics, EPR, or metal analysis.

Formation of Fe-Removed Reaction Centers (Apo-RCs). Deuterated RCs (described above) were incubated for 10 min

on ice with 4 mM *o*-phenanthroline, 0.1 mM EDTA, 20 mM Tris-HCl, and 3 equiv of deuterated ubiquinone-10. LiSCN was added to a final concentration of 1.5 M, and 1 volume of Chelex 100/2 volumes of protein solution was added. The mixture was tumbled for 60 min at room temperature. The Chelex 100 resin turned a pale pink color due to the binding of Fe−thiocyanate complexes. The protein was dialyzed overnight as detailed above. To reduce oxidized dimer (P_{865}^+), 0.2 mM sodium ascorbate was added, and the RCs were loaded onto a 1.5 mL DEAE-Sephacel column equilibrated with 10 mM Tris-HCl at pH 7.9, 0.01 mM EDTA, 60 mM NaCl, and 0.045% LDAO. The bound RCs were washed with 5 column volumes of buffer, eluted with 280 mM NaCl buffer, and cryogenically frozen.

For both the apo-RC and Zn-RC, three subunit protein bands were observed on a 12% SDS−PAGE gel with intensity ratios equivalent to those of the native RC (H-subunit stains ∼1.5-fold darker than the L- and M-subunits). Native agarose gels gave unreliable results. Nonetheless, if the H-subunit was not bound, the resulting LM complex would degrade rapidly with LDAO present (turning a green or gray color with high 280 nm/803 nm ratios) (Agalidis et al., 1987; Debus et al., 1985). The Zn-RCs and apo-RCs are a bright blue color, with the 280 nm/803 nm ratio essentially unchanged from the starting protein, and are very stable in LDAO. Protonated apo- and Zn-RCs were prepared under the same conditions.

Formation of Fe-Removed Reaction Centers without the H-Subunit (Apo-LM). Fe-removed LM complex was prepared based on a previously described method (Debus et al., 1985). Because the LM complex is unstable in LDAO, LDAO was removed by washing and eluting the RCs from the final DEAE-Sephacel purification step with buffers containing 0.8% *n*-octyl *β*-D-glucoside (OG) instead of LDAO. 2 mM *o*-phenanthroline and 4 equiv of deuterated ubiquinone-10 were added to deuterated RCs (1 mL; OD_{803} = 10−12 cm^{-1} in 10 mM Tris-HCl, pH 7.9, 0.01 mM EDTA, 280 mM NaCl, and 0.8% BOG) and dialyzed (10 mm wide 12 000−14 000 MWCO tubing) 60 min at room temperature against 10 mM Tris-HCl at pH 7.9, 0.01 mM EDTA, 0.8% OG, 2 mM *o*-phenanthroline, 10% ethanol, and 0.7 M $LiClO_4$. The protein was renatured by dialyzing 12 h against 10 mM Tris-HCl, pH 7.9, 0.01 mM EDTA, 0.8% OG, and 5 g of Chelex 100 resin at 4 °C. Precipitate was spun down, and the protein was frozen cryogenically and stored at −80 °C. Greater than 95% of the H-subunit was removed as shown by lack of the H-subunit protein band on 12% SDS−PAGE gels.

Metal Analysis: *ICP-AES and EPR Spectroscopy*. Direct measurement of Fe, Mn, and Zn contents was obtained using inductively coupled plasma-atomic emission spectroscopy (ICP-AES) on a Thermo Jarell Ash Auto Scan 25 spectrometer. ICP-AES enables rapid sequential multielement determination with minimal sample volume. The metal content of the RCs was analyzed before and after Fe removal. The Fe-removed samples were dialyzed against Chelex 100 resin for at least an additional 24 h prior to metal analysis.

Low-temperature Q-band (∼34 GHz) and X-band (∼9 GHz) EPR spectra were obtained to determine the amount of $P_{865}^+[Fe^{2+}Q_A]^-$ or $P_{865}^+Q_A^-$ formed under continuous illumination. The X-band data were collected using a Bruker ESP300E EPR, and the Q-band data were collected using a Varian E9 EPR spectrometer (Bruker Q-band bridge), as described previously (Feezel et al., 1989). The *g*-factors were determined by comparison to the light-induced signal of P_{865}^+ (g = 2.0026) in protonated native RCs of *Rb. sphaeroides* R-26. The dark signal before and after illumination was measured.

Measurement of k_Q. Transient absorption measurements of the room temperature kinetics of the pheophytin to Q_A electron transfer process were measured at the Bph anion band at 670 nm. The apparatus used for these experiments has been previously described (Greenfield et al., 1996). The RCs were excited at 595−597 nm with sub-200-fs pulses, and excitation energy densities were 200−500 $\mu J/cm^2$. Probe pulses were polarized at the magic angle to the pump, and a short-pass interference filter was used to eliminate the unconverted 820 nm light in the probe beam. Preliminary measurements at 12 K were obtained for frozen RC samples in 60% glycerol. The pump rate of the laser was slowed to 23 Hz for these experiments.

Time-Resolved EPR. The direct-detection time-resolved EPR experiment has been described (Stehlik et al., 1989; Trifunac et al., 1978). Transient EPR spectra were collected on a Bruker ESP300E spectrometer equipped with a low-temperature cryostat cooled to 12 or 70 K. An X-band ER046XK-T or a Q-band ER053QRD bridge was used. A home-built cylindrical Q-band cavity was constructed with silver wound wire to allow light into the cavity (M. D. E. Forbes, personal communication). The transient EPR signal was collected with narrow-band direct detection of the EPR signal with a Princeton Applied Research, Model 162, boxcar averager. Two separate 15 ns gates (a and b) were used to collect the (a) light-induced signal (1 μs after the laser flash) and (b) the dark background signal between laser pulses. The boxcar averager was run in the a−b mode while the magnetic field was scanned. Absorption (*A*) is plotted positive and emission (*E*) signals plotted negative. The samples were illuminated with 594 nm light from a Lumonics HyperDYE 300 dye laser pumped by a Questek 2040 XeCl excimer laser or with a nanosecond OPO laser system (Rainbow ω, OPOTEK Inc., Carlsbad, CA). The repetition rate was 10 Hz. A linear base line correction was applied to subtract the broad contribution of $^3P_{865}$ from the narrow $P_{865}^+Q_A^-$ signals when necessary.

Simulations. Spin levels with Boltzmann population were used to simulate $P_{865}^+Q_A^-$ spectra under continuous illumination. The features of these spectra are not sensitive to the structural differences reported for three crystal structures (Allen et al., 1988; Chang et al., 1991; Ermler et al., 1994). These features are dominated by the *g*-tensors for P_{865}^+ and Q_A^- and are influenced less by the relative orientation of the *g*-tensors with respect to the dipolar tensor of the electron−electron interactions.

The simulated time-resolved EPR spectra were obtained using the SETP model with the magnetic parameters listed in the previous work (Tang et al., 1996) and the X-ray structure data of the Argonne group (Chang et al., 1991). Two overlapping Gaussian functions were used to simulate the overall hyperfine couplings. The data were simulated using an isotropic *g*-value of 2.0035 for the Bph radical anion and τ_{PH} ($1/k_Q$) values in the range 0−6 ns. In order to obtain a good agreement between the experimental data and our "starting point" (fast k_Q) simulated spectrum, the relative Euler angle, ψ, for Q_A^- was rotated 15°. Using these Q_A^- coordinates for the τ_{PH} = 0 spectrum, the trends in spectral

changes as k_Q decreases are more readily comparable to the experimental trends. Difficulties in simulating X-band spectra have been attributed in part to exchange interactions (van den Brink et al., 1994), anisotropic hyperfine couplings (van der Est & Stehlik, 1996), or uncertainty in the quinone coordinates. For the higher microwave frequency Q-band data, the overlapping spectral features are resolved, and the simulation using a 15° rotation of the relative Euler angle ψ for Q_A^- still provides the best match to the experimental fast k_Q spectrum.

RESULTS

LiSCN-Based Iron-Removal Procedures. After many trials, we were unable to reproduce the Fe-removal procedures of Debus et al. (1986). One common problem was that the RCs aggregated or precipitated in the presence of 0.1% and 0.03% sodium cholate. This is not surprising as the CMC for cholate is 0.3% (Michel, 1991; Neugebauer, 1987). Most likely an unspecified amount of LDAO remained after the dialysis treatment of Debus et al. (1986) keeping the RC soluble, and this residual LDAO was critical for Fe-removal and H-subunit retention. This idea is substantiated by previous studies with ^{14}C-labeled LDAO-RCs that showed a large fraction of LDAO tightly bound to the RC, with only ~50% of LDAO removed after 4 days of dialysis against detergent-free buffer (Feher & Okamura, 1978). Apparently, completely LDAO-free RCs can be obtained only after stringent treatment with Bio-Beads (Bio-Rad) (Gast et al., 1994). We found that by starting with RCs purified in a low amount of LDAO, we could reproducibly prepare Fe-removed and Zn-replaced RCs. The RC did not degrade after chaotropic treatment with LiSCN in a LDAO-containing buffer. Apparently, the H-subunit does not completely dissociate from the L- and M-subunits. Thus, a concentration of 0.045% LDAO was low enough to retain the H-subunit and not harm LM after chaotropic treatment. The RC should be purified directly in 0.045% LDAO, and anion exchange chromatography performed such that peak fractions collected have RC concentrations of 60−70 μM. Fe-removal procedures using Centricon-50 (Amicon) concentrated RCs as the starting material produced inconsistent results (loss of H-subunit, no Fe-removal, etc.) because the LDAO concentration was altered by the concentration procedure. Simple dialysis against 0.045% LDAO buffer for purified RCs in buffers with different detergent compositions was not adequate to ensure repeatable Fe-removal procedures.

It is critical that the concentration of the LiSCN stock solution be determined by analytical analysis (i.e., ICP-AES, AAS) prior to protein addition. An excess of thiocyanate results in the loss of H-subunit concomitant with protein degradation. If the final thiocyanate concentration is too low, however, the Fe^{2+} will not be removed. Interestingly, complete Fe removal occurs in the absence of *o*-phenanthroline, as determined by EPR analysis (data not shown). Apparently *o*-phenanthroline does not chelate the Fe^{2+}. Instead, it is the formation of Fe−thiocyanate complexes that is critical for successful Fe removal. Fe−thiocyanate formation is consistent with the observed pink Fe-containing precipitate that forms after incubation of the protein with LiSCN. These thiocyanate complexes seemingly stick to the hydrophobic surface of the RC, because extensive Chelex resin treatment is necessary to remove excess Fe^{2+} from the RC. Both Zn-RC and apo-RC preparations have been successfully repeated at least 6 times each from three different batches of purified RCs.

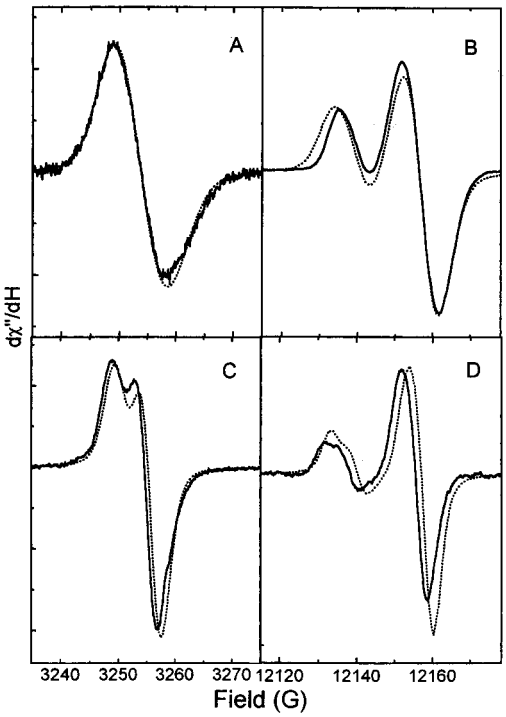

FIGURE 1: Experimental and simulated EPR data of protonated (A, B) and deuterated (C, D) Fe-removed RCs showing the $P_{865}^+Q_A^-$ charge-separated state. The EPR spectra were measured at 12 K under continuous illumination with a Xenon lamp. The X-band data were collected with 2 G (A) or 0.5 G (C) modulation amplitude, 126 μW microwave power, and 100 kHz field modulation using a Bruker ESP300E EPR spectrometer. The Q-band data were collected at 34 GHz, with 1.5 G (B) or 0.7 G (D) modulation amplitude, and 126 μW microwave power, using a Varian E9 EPR spectrometer with a Bruker Q-band bridge. The spectra shown are light minus dark signals. The simulated data (dashed lines) of the Boltzmann signals $P_{865}^+Q_A^-$ at X- and Q-band frequencies are shown for comparison.

Metal Content: EPR and ICP-AES Analysis. Light-induced EPR signals were obtained to directly determine the success of the three Fe-removal procedures. In native Fe-containing RCs, Q_A and Q_B are magnetically coupled to the Fe^{2+}. Upon illumination at 4 K, EPR signals are observed from the radical pair $P_{865}^+[Fe^{2+}Q_A]^-$. The *g*-value for P^+ is 2.0026, whereas $[Fe^{2+}Q_A]^-$ gives rise to a broad resonance centered at ~1.8 (Feher, 1971; Loach & Hall, 1972). In the absence of the paramagnetic metal, the quinone signal narrows to that of a typical organic radical with $g = 2.0049$. In protonated samples at X-band, the Boltzmann signals from P_{865}^+ and Q_A^- overlap, resulting in a derivative signal at $g = 2.0037$ (Debus et al., 1986) that is asymmetric (less intense and broader at high field than low field) (Figure 1A). These overlapping resonances are resolved at higher fields and upon deuteration (Feher et al., 1972; Feezel et al., 1989). Thus, for Fe-removed RCs, both P_{865}^+ and Q_A^- resonances are observed for deuterated RCs at X-band (Figure 1C) and for both protonated (Figure 1B) and deuterated RCs (Figure 1D) at Q-band. Less direct EPR methods to determine the lack of Fe^{2+} include monitoring the absence of the $[Fe^{2+}Q_A]^-$ signal (van den Brink et al., 1994) or observing an emissively polarized Q_A^- EPR signal from illumination of a dark Q_A^- EPR signal (Gast & Hoff, 1979; Hoff & Gast, 1979). If

Table 1: Metal-to-Protein Ratios Determined by ICP-AES Analysis of Various Preparations of *Rb. sphaeroides* RCs[a]

sample	Fe/RC	Mn/RC	Zn/RC	no. of samples
purified R26	0.46 ± 0.14	0.58 ± 0.09	0.30 ± 0.30	14
Chelex-treated purified R26[b]	0.58 ± 0.08	0.63 ± 0.05	<0.02	4
apo-RC[c]	0.33 ± 0.10	0.17 ± 0.10	0.24 ± 0.14	4
Zn-RC[c]	0.20 ± 0.09	0.06 ± 0.05	0.85 ± 0.22	8

[a] Standard deviations listed are for sample-to-sample variations resulting from differences between separate preparations. The actual analytical standard deviation for each individual measurement was less than 0.01. [b] The protein was treated with Chelex 100 (Bio-Rad) chelating ion exchange resin. [c] These samples were extensively Chelex-treated prior to metal analysis. Without this Chelex treatment, the metal: protein ratios were essentially unchanged from the purified R26 values, even though EPR analysis showed that the Fe and Mn were uncoupled from the quinone.

Mn^{2+} were in the Fe-site, however, the $[Fe^{2+}Q_A]^-$ signal would not be observed (Rutherford et al., 1985). Here we present an alternate more direct EPR method for determining metal content: comparison of the experimental $P_{865}{}^+Q_A{}^-$ signals to simulated $P_{865}{}^+$ and $Q_A{}^-$ signals expected for total paramagnetic metal ion depletion. The experimental data show good agreement to the calculated EPR spectra, indicating that essentially complete Fe removal was obtained with each of the three protocols. Thus, excess $P_{865}{}^+$ signal as $P_{865}{}^+[Fe^{2+}Q_A]^-$ at $g = 1.8$ is not an issue for these samples and will not influence the observed ESP signals around $g = 2.0$.

Table 1 shows the Fe, Mn, and Zn contents of the RCs before and after Fe-removal procedures determined by ICP-AES analysis. The standard deviations listed show the sample-to-sample variation between individual protein preparations. ICP-AES measurements are very accurate for metal concentrations >100 ppb, with standard deviations less than 3% of the measured value. Unexpectedly, ICP-AES analysis of *Rb. sphaeroides* R-26 showed that our purified RCs contain a significant amount of manganese. Mn-to-RC ratios of ~0.6 and Fe-to-RC ratios of ~0.5 were measured from 10 different purified preparations of RCs. Like Fe^{2+}, the paramagnetic Mn^{2+} in the RC is magnetically coupled to the quinone (Rutherford et al., 1985). Not surprisingly, the Fe-removal procedures also removed the Mn^{2+}, as determined by the observed $P_{865}{}^+Q_A{}^-$ EPR signals showing that Mn^{2+} and $Q_A{}^-$ were uncoupled. In some preparations, extraneous iron was observed. Weakly bound adventitious Fe^{2+} was removed prior to ICP-AES analysis by size-exclusion chromatography with Sephadex G25.

The Mn and Fe contents of the RCs determined by ICP-AES analysis after Fe-removal procedures without Chelex treatment were puzzling. The metal-to-protein ratios of the RCs before and after metal removal were essentially the same, although EPR analysis indicated that the paramagnetic metal ions were uncoupled from the quinone. Only after extensive dialysis vs Chelex 100 resin was the total Fe plus Mn content-to-protein ratio substochiometric (Table 1). Apparently, after LiSCN treatment, the Fe and Mn ions are surface-bound and accessible to Chelex resin. The same Chelex treatment does not remove Fe, Mn, or Zn from the buried Fe-site in native RCs. Even after extensive Chelex treatment, the metal-to-protein ratios for Fe-removed RCs can be misleading. The remaining ~30% Fe is most likely residual surface-bound based on EPR results (Figure 1). Thus, the light-induced $P_{865}{}^+Q_A{}^-$ EPR signal was found to be a more reliable method for determining the extent of paramagnetic metal removal than ICP-AES analysis.

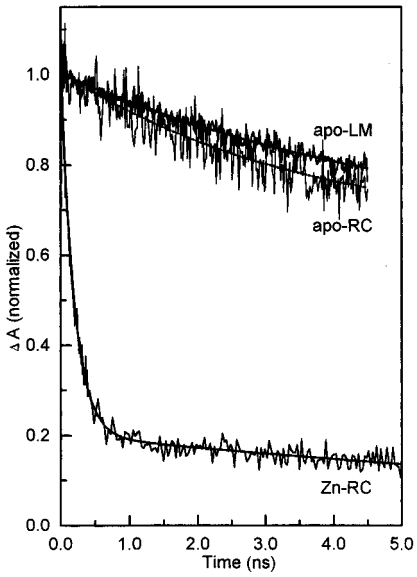

FIGURE 2: Transient absorption measurements and fits of Fe-removed RCs showing the kinetics of the Bph → Q_A electron transfer process measured at the Bph anion band at 670 nm. The RCs were excited at 595−597 nm with sub-200 fs pulses. The measurements were taken at ~295 K. The decays for Zn-RC were fit to a ca. 200 ps component (fast k_Q) and a >10 ns component. The decays of the apo-RC and apo-LM did not require the fast component.

Interestingly, purified RCs contain a significant amount of Zn^{2+}. As shown in Table 1, purified RCs prior to Fe-removal treatments have on average 0.3 Zn^{2+} per RC. We have observed anywhere from 0 to 1 Zn^{2+} per RC without addition of extra Zn^{2+}. RCs that have been incubated with several equivalents of Zn^{2+} followed by size-exclusion chromatography have close to stoichiometric Zn binding. Q-band EPR analysis of these RCs with 1 Zn/RC (Fe and Mn not removed) confirms that this Zn^{2+} is not bound in the Fe-site. A $Q_A{}^-$ signal is not observed in the $g = 2.0$ region. Treatment with Chelex 100 resin removes this extra Zn^{2+}, suggesting that the Zn^{2+} is binding near the surface of the protein. Elaboration of these results will be presented in a future paper (L. M. Utschig and D. M. Tiede, unpublished results). This "adventitious" Zn-site on the RC complicates experiments involving insertion of Zn^{2+}, or other metal ions, into the Fe-site. Previous methods (Debus et al., 1986) involve incubation of Fe-removed RCs with large quantities of Zn^{2+}, or other transition metal ions, followed by dialysis. Based on our results, it is possible that these transition metal ions do not bind in the Fe-site, but rather bind to other surface-accessible site(s). Therefore, when simply reporting Zn-to-RC ratios, it is important to determine if the Zn^{2+} is in the Fe-site by determining these ratios after extensive Chelex treatment and by examination of EPR spectra.

Electron Transfer from BPh to Q_A. Figure 2 compares the room temperature kinetics of the Bph → Q_A electron transfer process (k_Q) measured by transient absorption spectroscopy at the 670 nm Bph anion band for apo-RCs, Zn-RCs, and apo-LM. Native RCs have a k_Q of ~$(200\ ps)^{-1}$ (Kirmaier et al., 1985). The majority of the decay (80%)

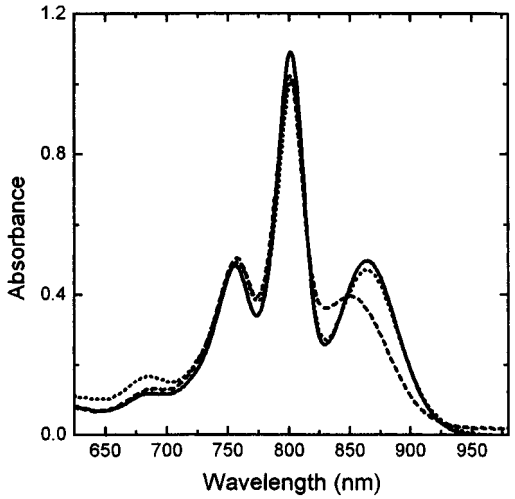

FIGURE 3: Dependence of the position of the long-wavelength absorption (near 865 nm) on the Fe-removal procedures and resulting k_Q. A 15−20 nm blue shift and a decrease in intensity of the 865 nm P_{865} peak were routinely observed after the Fe-removal procedures for Fe-depleted samples where k_Q is slow (apo-RC shown here, dashed line). For Zn-RCs where k_Q is fast (dotted line), the intensity and position of this peak remained essentially unchanged relative to those observed for native RCs (solid line).

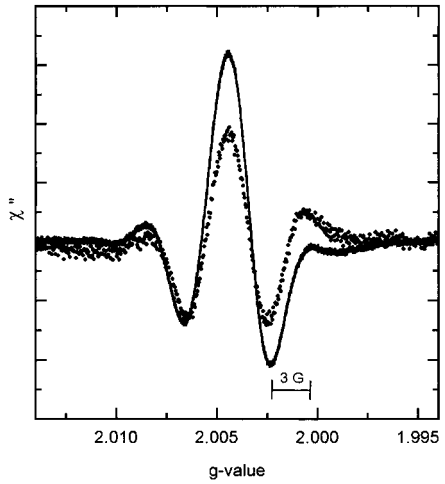

FIGURE 4: Experimental X-band ESP EPR spectra of $P_{865}{}^{+}Q_A{}^{-}$ of deuterated Fe-removed bacterial RCs with fast or slow k_Q in frozen solution at 12 K. The sweep width was 50 G, the microwave power was 1 mW, and 5 scans were averaged. The Zn-RCs and apo-RCs were prepared as detailed in the text, concentrated to $OD_{800} = 25$ cm^{-1} and 10 cm^{-1} with A_{280}/A_{800} ratios of 1.4 and 1.5, respectively, and cryogenically frozen after dark-adaptation. The spin-polarized spectrum for Zn-RCs with ∼80% $(200\ ps)^{-1}$ k_Q is shown in boldface, and the corresponding spectrum for apo-RC with $(3-6\ ns)^{-1}$ k_Q is dotted. The transient optical data for these samples are shown in Figure 2, and the EPR signals under continuous illumination of Zn-RCs are essentially identical to those of apo-RCs shown in Figure 1C,D.

for Zn-RCs was fit to a fast 200 ps component, with the remaining amplitude (20%) belonging to an additional >10 ns decay component. 545 nm data (not shown), corresponding to the decay of the Bph Q_x bleach, are consistent with the 670 nm data. The ∼5 ns maximum delay of the apparatus precludes the accurate determination of a many-nanosecond time constant. The nanosecond decay component is residual Bph anion at long time. It could result from inactive RCs which lack a functional quinone acceptor (Liu et al., 1991), which is consistent with small $^3P_{865}$ triplet EPR signals observed under continuous illumination at 4 K. The fits to the decay curves of the apo-RC with and without the H-subunit did not require the fast component, with the best fit to the data yielding a slow 3−6 ns component (Kirmaier et al., 1986; Liu et al., 1991) and a nondecay component. The triplet yield was high in these samples, as measured qualitatively by EPR. Preliminary measurements indicate that the k_Q for the slow component increases to approximately $(1.5-2.0\ ns)^{-1}$ at 12 K. The rate for the appearance of the Bph anion band was typically $(3.5-4.0\ ps)^{-1}$. The kinetics of the apo- and Zn-RCs were remeasured after the EPR experiments, 4 months after their preparation and storage at 77 K. No significant change in the quantity or rate of fast component for Zn-RC was observed. The slow component for apo-RC and apo-LM did not appear to significantly change over time, within the error of the experiment.

A change in the visible absorption spectrum is strongly correlated to the slow k_Q (Figure 3). A 10−15 nm blue shift and reversible bleaching of the 865 nm peak of the special pair P_{865} were routinely observed for apo-RC and apo-LM samples where k_Q is slow. For Zn-RC samples where k_Q is fast, the intensity and position of this peak remained essentially unchanged relative to those observed for native RCs. Zn substitution into the Fe-site, however, does not assure retention of the native k_Q. In the process of developing a reliable preparation of fast $(200\text{-ps})^{-1}$ k_Q Zn-RCs (detailed above), we prepared several Zn-RC samples that had a predominant slow k_Q rate. Apparently, it is very difficult to not alter the protein during Fe removal and retain the native k_Q of $(200\ ps)^{-1}$.

Time-Resolved EPR. The amount of uncoupled quinone will influence the relative intensities of ESP resonances observed in the $g = 2$ region for the light-induced charge-separated state. Upon illumination, the relative amounts of $Q_A{}^{-}$ to $P_{865}{}^{+}$ resonances of the X-band and Q-band CW EPR signals were equivalent for the deuterated apo-RC, Zn-RC, and apo-LM samples. Each sample used in the time-resolved experiments had essentially complete Fe^{2+} and Mn^{2+} removal. The samples were checked for the presence of any reduced quinone in the dark before and after illumination, since spin-polarized signals from chemically prereduced RCs (Gast & Hoff, 1979; Hoff & Gast, 1979) have been observed in such systems and could interfere with the ESP spectrum of $P_{865}{}^{+}Q_A{}^{-}$. All three samples had negligible dark signals before and after illumination.

The X-band transient EPR spectra of kinetically-defined deuterated Zn-RCs and apo-RCs, with fast k_Q and slow k_Q, respectively, are shown in Figure 4. These spectra are not corrected for concentration, and therefore the overall intensities between spectra cannot be compared. The spectra for both have an (*A*)/*E*/*A*/*E*/(*A*) polarization pattern (E = emission, A = absorption). These spectra are highly resolved for X-band frequency and have a similar polarization pattern as previously observed with protonated Zn-RCs at K-band frequency (∼24 GHz) (Füchsle et al., 1993; van der Est, 1995). The most striking difference between the two spectra presented in Figure 4 is the relative intensity of the polarized resonances within each spectra. For apo-RCs, the absolute amplitudes of the (*A*)/*E*/*A*/*E*/(*A*) lobes have an approximately (0.2)/1/1.3/1/(0.5) relative intensity ratio. The high- and low-field emissions have the same absolute amplitude with the central absorption only slightly more intense than either emission. The Zn-RCs, however, have a high-field emission

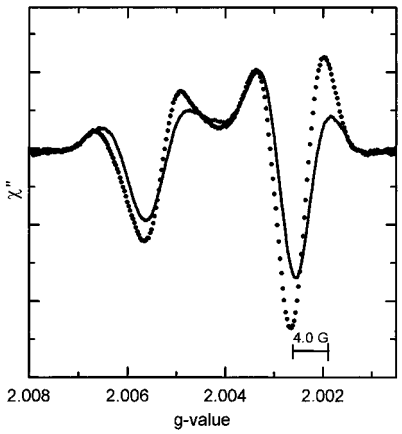

FIGURE 5: Experimental Q-band ESP EPR spectra of $P_{865}^{+}Q_A^{-}$ of deuterated Fe-removed bacterial RCs with fast or slow k_Q in frozen solution at 70 K. The sweep width was 50 G, the microwave power was 2 mW, and 5 scans were averaged. The Zn-RCs and apo-RCs samples are described in Figure 4. The spin-polarized spectrum for Zn-RCs with ~80% (200 ps)$^{-1}$ k_Q is shown in boldface, and the corresponding spectrum for apo-RC with (3−6 ns)$^{-1}$ k_Q is dotted.

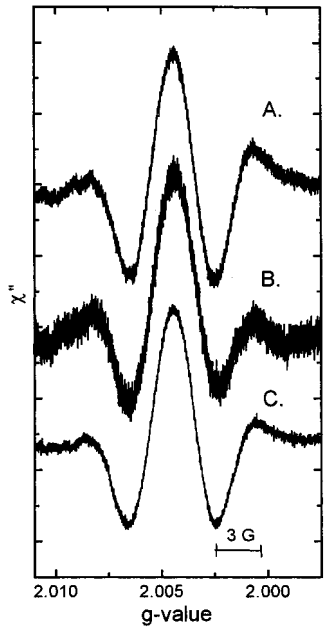

FIGURE 6: Comparison of the X-band $P_{865}^{+}Q_A^{-}$ ESP signals of apo-RC, apo-LM, and Zn-RC samples with slow k_Q. The spectra of (A) apo-RCs (described in Figure 4), (B) apo-LM (OD_{800} = 14 cm^{-1}, A_{280}/A_{800} = 1.4), and (C) Zn-RCs with slow k_Q were obtained at 12 K as described in Figure 4, except 10 scans were averaged for the apo-LM spectrum. The Zn-RC sample in this preparation was prepared differently than described in the text. The RC was incubated with 1.5 M LiSCN for 40 min at 25 °C prior to the addition of 0.5 mM $ZnSO_4$ and 5 mM 2-mercaptoethanol. After an additional 25 min at room temperature, the protein was dialyzed overnight. The P_{865} absorbance maximum shifted to 855 nm after preparation. This Zn-RC EPR sample had OD_{800} = 18 cm^{-1} and A_{280}/A_{800} = 1.2. The Boltzmann EPR signal was essentially identical to those in Figure 1C,D and the kinetic trace matched that of apo-RC shown in Figure 2. No fast k_Q component (<10%) was observed. The transient optical data for apo-LM are shown in Figure 2.

more intense than the low-field emission, as well as a high absolute central absorption, with an approximate ratio for these dominant *E*/*A*/*E* lobes of 1/2.3/1.6. The small absorption at high field is below the base line and is much less predominant and at a slightly lower *g*-value than that observed for apo-RCs. Also, the magnetic field separation between the two emissive lobes narrows by 0.8 G for apo-RCs. Another feature of the Zn-RC spectrum is a weak emission at the highest field. The origin of this feature is unclear (van der Est et al., 1993). These polarization patterns were observed for two different deuterated preparations of kinetically defined fast k_Q and slow k_Q samples. No significant change in the shape or relative intensities of the X-band ESP spectra for apo-RCs in the temperature range of 12−180 K was observed.

Figure 5 shows the transient spectra obtained at Q-band for deuterated apo-RCs with slow k_Q and for Zn-RCs with fast k_Q. These spectra are highly resolved, and, in fact, exhibit similar spectral resolution as protonated Zn-RCs at W-band (Prisner et al., 1995). A polarization pattern of (*A*)/*E*/*A*/*A*/*E*/*A* is observed for both spectra. As observed for X-band, the major difference between the Q-band spectra is also the relative intensity of the polarized resonances within each spectra. The absolute amplitudes of the (*A*)/*E*/*A*/*A*/*E*/*A* lobes are approximately (0.2)/1/0.6/0.8/1.9/1 and (0.3)/1/0.5/1/1.7/0.4 for apo-RCs and Zn-RCs, respectively. Moreover, the high-field emission and absorption for apo-RCs are at slightly higher *g*-values than those observed for Zn-RCs. Clearly, the high-field region of the polarized spectrum is influenced the most by the different k_Q values, although slight differences are observed in the low-field region. The high resolution at Q-band for deuterated Fe-removed samples partly separates the contributions of the radicals P_{865}^{+} and Q_A^{-} to the overall polarized spectrum (Feezel et al., 1989). Changes in the orientation of P_{865}^{+} relative to the dipolar vector joining the two radicals primarily affect the high-field region, whereas changes in the orientation of Q_A^{-} principally affect the low-field part of the spectrum (van der Est et al., 1996). Therefore, the Q-band spectral results indicate that the P_{865}^{+} region is affected more than the Q_A^{-} part when k_Q is slow. The extent to which these changes can be attributed to a contribution from the intermediary radical pair $P_{865}^{+}H^{-}$, which would be expected to overlap the high-field region, or to actual structure changes in the cofactors will be investigated by comparison to simulated data.

The observed relative intensity differences in polarization patterns are correlated to the amount of slow and fast components and not specifically to metal content. Prior to development of the refined fast k_Q Zn-RC procedure (detailed above), the majority of our Zn-RC preparations were found to have a slow (3−6 ns)$^{-1}$ k_Q. The X-band and Q-band ESP spectra for one of these Zn-RC samples prepared with "harsher" conditions (described in the figure caption) are shown in Figures 6C and 7B, respectively. Interestingly, this slow k_Q Zn-RC sample exhibits an almost identical spin-polarized spectrum to that of apo-RCs. Likewise, Zn-RC samples with a combination of fast and slow kinetic components exhibit spectra intermediate with respect to the changes described above for signals obtained for samples with a predominant slow or fast kinetic component. Thus, the method of sample preparation and resulting kinetics will influence the observed transient EPR spectra. Many published experimental spin-polarized X-band spectra for Zn-RCs have been obtained with samples that have not been kinetically characterized (Feezel et al., 1989; van der Est et al., 1993, 1995; Bittl et al., 1994, 1996; Kothe et al., 1994). Our results suggest that differences between these spectra could reflect differences in kinetics of the samples.

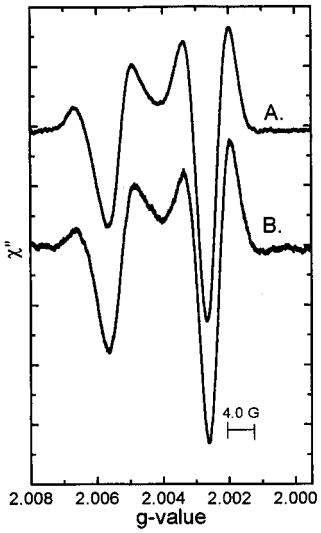

FIGURE 7: Comparison of the Q-band $P_{865}{}^{+}Q_A{}^{-}$ ESP signals of apo-RC and Zn-RC samples with slow k_Q. The spectra of (A) apo-RCs (described in Figure 4) and (B) Zn-RCs with slow k_Q (described in Figure 6) were obtained at 70 K as described in Figure 5.

A comparison of the ESP EPR spectra of Fe-removed RC with or without the H-subunit is shown in Figure 6A,B. Both samples were kinetically identical, having slow $(3-6\ \text{ns})^{-1}$ k_Q rates. Each spectrum has the overall (*A*)/*E*/*A*/*E*/(*A*) spin polarization pattern. The high-field emission is slightly less intense than the low-field emission in the apo-LM protein. The apo-LM protein had a larger underlying triplet $^3P_{865}$ signal than the apo-RC, most likely due to a high loss of weakly bound quinone because of the lack of H-subunit. A linear base line correction was applied to each spectrum to account for the underlying triplet signals.

Simulated ESP Spectra. To investigate the differences observed in the experimental spectra, the influence of the rate k_Q on the polarization pattern was examined. ESP EPR spectra were simulated using the cofactor coordinates from the X-ray structural data of the Argonne group (Chang et al., 1991) and magnetic parameters listed previously (Tang et al., 1996). The spectra can be described by the CRPP model (Fåchsle et al., 1993; van der Est et al., 1993) for systems where the lifetime of $P_{865}{}^{+}H^{-}$ is 200 ps, as in native RCs and Zn-RCs. However, the simulations presented here are based on a more general model, the SETP model (Norris et al., 1990; Morris et al., 1995; Tang et al., 1996), which takes into account the effects of a long-lived intermediate electron acceptor when the electron transfer to Q_A is slowed.

In Figure 8, the simulated X-band and Q-band SETP spectra are shown for 0−6 ns lifetimes, τ_{PH}, of the intermediary radical pair $P_{865}{}^{+}H^{-}$. The trends for systematically increasing the lifetime of $P_{865}{}^{+}H^{-}$ provide information about the importance of including the intermediate radical pair. These simulations are applicable to the apo-RC and apo-LM, where τ_{PH} $(1/k_Q)$ was measured to be 3−6 ns at room temperature. Figure 8 shows that, as the rate k_Q becomes slower, the high-field (*A*) increases in size with an apparent shift to higher *g*-value and concomitant loss of relative amplitude of the high-field emission and central absorption. Also, the magnetic field separation between the two emissive lobes decreases as the rate slows down. These trends in the simulated polarized spectra match those discussed above for the experimental spectra in Figures 4 and 5. The extent of

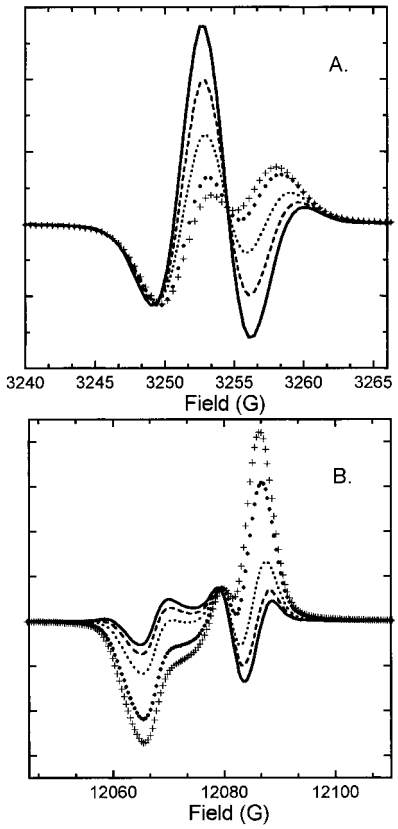

FIGURE 8: Simulated (A) X-band and (B) Q-band EPR spectra of deuterated Fe-depleted RCs with varying k_Q showing the trend for increasing involvement of the intermediate radical pair $P_{865}{}^{+}H^{-}$ on the observed spectrum. The SETP model was used with an isotropic *g*-value for the Bph anion and τ_{PH} values of 0, 1, 2, 4, and 6 ns (solid, dashed, dotted, circle, and plus, respectively).

the change for the experimental spectra, however, does not match that observed in the 4 ns or 6 ns simulated spectra. One possible explanation for this is that k_Q is faster at liquid He temperatures than at room temperature. Preliminary k_Q optical measurements at 12 K show that the rate does in fact increase to about $(1.5-2\ \text{ns})^{-1}$ at this temperature for apo-RCs. Apparently, the k_Q for slow RCs is still at least 15-fold slower at 12 K than for RCs with the native k_Q which have been reported to have k_Q of ∼100 ps at this temperature (Kirmaier et al., 1985).

Although the 1 ns and 2 ns simulated spectra closely resemble the experimental spectra for the slow k_Q RCs, differences still exist. Actual fitting of the experimental spectra will address whether or not these changes are due to structural differences in $P_{865}{}^{+}$, $Q_A{}^{-}$, or H^{-}, or if they can predominantly be explained by the differences in k_Q. Simulated spectral features are strongly influenced by the value and orientation of the *g*-tensor for the intermediate acceptor as well as the dipolar tensor between $P_{865}{}^{+}$ and $Q_A{}^{-}$. Although the *g*-tensors for $P_{865}{}^{+}$ and $Q_A{}^{-}$ are characterized (Burghaus et al., 1993; Isaacson et al., 1995; Klette et al., 1993), the corresponding values for the intermediate Bph acceptor have not been definitively determined. Recently, the ESP signal of the primary radical pair $P_{865}{}^{+}H^{-}$ has been reported (Proskuryakov et al., 1996), and further studies of this signal will provide important magnetic parameters of this species.

DISCUSSION

Fe-Removal Procedures. In this study, we examined the ESP EPR spectra of three different preparations of RCs from *Rb. sphaeroides* R-26 depleted of Fe^{2+} where the electron transfer rate from the bacteriopheophytin to the quinone acceptor has been measured. Transient EPR signals were found to be very preparation- and k_Q-dependent. Unexpectedly, we encountered difficulties repeating previous literature procedures for Fe-removal with H-subunit retention (Debus et al., 1986) and observed a different correlation between the specific protein modification and corresponding k_Q rate. Importantly, Zn^{2+} substitution for the Fe^{2+} or a combination of Fe-depletion and H-subunit removal does not assure retention of the native $(200\ ps)^{-1}$ k_Q electron transfer rate. This native rate was only observed for Zn-RCs that had been prepared in a precise manner, with time-specific addition of zinc sulfate to a reaction mixture of chaotrope LiSCN with *o*-phenanthroline, 2-mercaptoethanol, and ubiquinone. Irreversible protein changes apparently occur with preparation of the apo-RCs with slow k_Q as we were unable to regain the native electron transfer rate by first preparing the apo-RC and later reconstituting with Zn^{2+} (Debus et al., 1986). Extraneous Zn^{2+} can bind to the surface of the RC by this method, and metal analysis would provide misleading information about the amount of Zn^{2+} substituted into the Fe site. Continuous light-induced $P_{865}{}^+Q_A{}^-$ EPR signals provided a good method for determining the success of the Fe-removal procedures.

Influence of k_Q on ESP EPR Spectra. With these kinetically-characterized proteins, we are able to directly investigate the influence of the intermediary $P_{865}{}^+H^-$ radical pair on the observed ESP signal of the $P_{865}{}^+Q_A{}^-$ radical pair. The use of deuterated protein provides higher spectral resolution of the overlapping $P_{865}{}^+Q_A{}^-$ resonances at X-band and Q-band (Feezel et al., 1989) by reducing the nuclear hyperfine interactions compared to analogous protonated RCs (Feezel et al., 1990). The sequential electron transfer polarization (SETP) model has been used to account for differences in the polarization line shape of $P_{865}{}^+$ in Fe-containing protonated *Rb. sphaeroides* with different quinones as Q_A (Morris et al., 1995), but has never before been applied to ESP spectra of $P_{865}{}^+Q_A{}^-$ from kinetically-defined deuterated Fe-removed RCs. With the SETP model, the ESP EPR spectrum is influenced by whether or not the ESP of the $P_{865}{}^+Q_A{}^-$ radical pair is affected by radical pair interactions of the precursor, $P_{865}{}^+H^-$ (Norris et al., 1990; Morris et al., 1995; Tang et al., 1996). In SETP simulations, the singlet-triplet mixing developed in the intermediate radical pair $P_{865}{}^+H^-$ is projected onto the correlated radical pair polarization (CRPP) developed on the final radical pair $P_{865}{}^+Q_A{}^-$.

In apo-RCs, the lifetime of $P_{865}{}^+H^-$ is longer by a factor of at least 15 relative to its lifetime in native RCs. The ESP signal of apo-RCs has a different spin-polarized spectrum than that of Zn-RCs which have a k_Q unchanged from native RCs and an ESP the result of the CRPP mechanism. These observed spectral differences reflect the trends in polarization predicted with the SETP model, verifying that the sequential nature of the electron transfer process contributes to the spin polarization in Fe-depleted RC preparations having a slow k_Q. The $P_{865}{}^+H^-$ lifetime in native RCs is only 2 times shorter at 5 K than at 295 K (Kirmaier et al., 1985), and the slow k_Q does exhibit a similar temperature dependence to native RCs, as preliminary optical measurements indicate that the slow k_Q rate increases to approximately $(1.5-2\ ns)^{-1}$ at 12 K. Interestingly, the experimental spectrum for apo-RCs is remarkably similar to the 1 ns and 2 ns simulated data, although differences do exist. Ultimately, least-squares fitting of the experimental spectra will provide essential information about whether these changes observed in the spectra can be attributed to structural differences in $P_{865}{}^+$, $Q_A{}^-$, or H^-, or if they predominantly can be explained by the differences in k_Q. Nevertheless, our results strongly suggest the need to consider both $P_{865}{}^+H^-$ and $P_{865}{}^+Q_A{}^-$ radical pair interactions in the interpretation of the ESP EPR spectra obtained from photosynthetic systems.

Because the observed spin polarization is dependent on k_Q, it is imperative to ascertain the k_Q rates of modified protein samples prior to detailed analysis of spin-polarized spectra. Contrary to previous ideas, simple substitution of Zn^{2+} into the Fe site does not assure that the native electron transfer rate has been retained. It is possible that a decrease in k_Q could explain some of the discrepancies observed in the high-field absorption and overall relative absolute intensities of published experimental spin-polarized X-band spectra for Zn-RCs (van der Est et al., 1993, 1995; Bittl et al., 1994, 1996; Feezel et al., 1990; Kothe et al., 1994). The differences in spectral shape due to slow vs fast k_Q are resolved at Q-band. The ESP spectrum of the deuterated Zn-RCs at Q-band provides similar resolution to the spectrum obtained with protonated Zn-RCs at W-band (Prisner et al., 1995). Our Q-band spin-polarized spectrum of deuterated Zn-RCs with native k_Q differs from the W-band results most dramatically in the high-field region of the experimental spectrum. Because of reproducibility problems with Fe-removal preparations and resulting "delicate" protein, RCs could have slow k_Q after further quinone extraction and replacement of Q_A with various quinones (van der Est et al., 1995). The concomitant measurements of ESP spectra and k_Q for Fe-removed RCs reported herein provide the first step toward definitively determining if light-induced structural changes in P_{865} or Q_A relative to the ground-state X-ray structure occur upon formation of the charge-separated state $P_{865}{}^+Q_A{}^-$.

Protein Modifications and Electron Transfer. Both transient EPR and optical spectroscopic data suggest that the slow k_Q in Fe-depleted RCs is H-subunit independent. Previously, a decay time of 200 ps for the apo-LM complex, indistinguishable from that measured for native, RCs has been reported (Blankenship & Parson, 1979; Agalidis et al., 1987; Liu et al., 1991). We never observed this. In fact, we found that it was relatively easy to make Fe-removed proteins with or without the H-subunit in the absence of Zn^{2+} that had a slow nanosecond k_Q electron transfer rate. This result contradicts previous reports. In *Rb. sphaeroides* wild type (Y strain) in which only the L and M protein subunits are present (metal depleted) (Agalidis et al., 1987) and in Fe-depleted $LiClO_4$-treated (Debus et al., 1985; Liu et al., 1991) or SDS-treated (Blankenship & Parson, 1979) RCs from *Rb. sphaeroides* R-26, the lifetimes of $P_{865}{}^+H^-$ are reported to be the same as that in native RCs. The reasons for the discrepancy of our data with previous data are unclear. The fact that slow kinetics can occur whether or not the H-subunit is present, however, implies that this alteration in electron transfer rate is not the direct result of H-subunit

removal. These results negate the suggestion that the H-subunit is specifically involved in a "spring-mechanism", shifting the Q_A orientation and causing slow k_Q (Liu et al., 1991; Schelvis et al., 1992).

Another interesting observation is that Zn^{2+} occupancy of the Fe site does not assure retention of native k_Q. All apo-RCs and some Zn-RCs had slow k_Q; and these samples exhibit almost identical spin-polarized signals (Figure 6). Transient EPR signals are sensitive to the orientation of the radicals, P_{865}^+ and Q_A^- (Fåchsle et al., 1993; Snyder & Thurnauer, 1993; van der Est et al., 1993, 1995; Prisner et al., 1995), and possibly to H^-. Therefore, apparently no major change in the orientation of these cofactors, as reflected in their magnetic parameters, occurs between apo-RCs, apo-LMs, and slow k_Q Zn-RCs, because all three exhibit strikingly similar spin-polarized signals. This suggests that the observed slow k_Q is not specific for either metal-site occupancy or H-subunit retention.

Not only might the slow k_Q be the result of structural changes in the quinone region, but also it could be the result of an altered orientation of the special pair P_{865}. The Fe-removal procedures induce a 10−15 nm blue shift in the P_{865} 865 nm absorption band for apo-RC and apo-LM. This shift was consistently observed for samples that had a major nanosecond k_Q component. One possible explanation for this absorbance shift is a loss of Q_B (Debus et al., 1985), but this does not appear to be a predominant factor for our samples because we observe a majority of Q_A to Q_B electron transfer (L. M. Utschig and D. M. Tiede, unpublished results). A similar shift has been observed with detergent-stripped RCs (Gast et al., 1996) and for RCs from certain species of purple bacteria with the dimer band reversibly shifting by the addition of charged detergents (Wang et al., 1994). Spectroscopic results indicate distinct differences in the electronic structure asymmetry for P_{850} and P_{865} (Rautter et al., 1994; Wang et al., 1994; Müh et al., 1996). Possibly, the slow k_Q for apo-RCs and apo-LM which have an 850 nm absorbance band could be attributed to a different spin density distribution for P_{850}^+ than the P_{865}^+ observed for Zn-RCs with native k_Q. The different electronic configuration could result from structural changes in the protein matrix due to Fe-removal or chaotropic treatment. The Q-band ESP spectra would support this hypothesis as the largest differences between the slow and fast k_Q samples occur in the high-field P_{865}^+ region of the spectrum.

In summary, we can reproducibly prepare well-characterized Fe-removed RCs with specific H^- to Q_A electron transfer rates and have obtained highly resolved X- and Q-band ESP EPR spectra with these samples. Distinct differences in the spin-polarized spectra are observed for apo-RCs having a >15-fold slower k_Q than Zn-RCs with native k_Q. These experimental results provide the essential foundation for determining the critical factors that influence this electron transfer process. Both ESP EPR and optical results indicate that the observed slow k_Q rate in Fe-removed RCs is H-subunit independent and, in some cases, independent of Fe-site occupancy as Zn substitution does not ensure retention of the native k_Q. Furthermore, shifts in the optical spectrum of P_{865} and differences in the high-field region of the Q-band spectrum for apo-RCs with slow k_Q indicate possible structural changes in the primary donor. Thus, Fe removal might induce structural changes in the quinone region or even induce changes at a distance by altering the relative orientations of Bph or special pair P_{865}. However, it is possible that a distinct cofactor adjustment does not occur as the direct result of removing specific Fe^{2+} or H-subunit interactions and that the observed differences can be accounted for simply by the change in kinetics. Thus, protein reorganization energy might play the major role in controlling the H^- to Q_A electron transfer process. This result would be consistent with other experiments that have shown large changes in $P_{865}^+Q_A^-$ recombination or Q_A^- to Q_B electron transfer rates can occur without large changes in the donor/acceptor geometries (Franzen et al., 1990; van den Brink et al., 1994; Tiede et al., 1996). Likewise, Fe^{2+} and/or H-subunit removal might affect global protein structure and dynamics. To address these possibilities, we have also obtained high time resolution transient EPR spectra of the apo-RC and Zn-RC and currently are analyzing the observed oscillations due to zero quantum coherence to determine donor/acceptor geometries (Kothe et al., 1994). The results from these studies combined with detailed SETP modeling of the observed ESP signals will provide essential information about whether the changes observed in the ESP spectra for samples with fast and slow k_Q can be attributed to structural differences in P_{865}^+, Q_A^-, or H^-, or if they predominantly can be explained by the differences in k_Q.

ACKNOWLEDGMENT

We thank T. Rajh, D. M. Tiede, A. Wagner, and G. Kothe for technical assistance and helpful discussions and J. R. Norris for the use of his Q-band bridge.

REFERENCES

Agalidis, I., Nuijs, A. M., & Reiss-Husson, F. (1987) *Biochim. Biophys. Acta 890*, 242−250.

Allen, J. P., Feher, G., Yeates, T. O., Komiya, H., & Rees, D. C. (1988) *Proc. Natl. Acad. Sci. U.S.A. 85*, 8487−8491.

Bittl, R., van der Est, A., Kamlowski, A., Lubitz, W., & Stehlik, D. (1994) *Chem. Phys. Lett. 226*, 349−358.

Bittl, R., Zech, S. G., & Lubitz, W. (1996) in *The Reaction Center of Photosynthetic Bacteria* (Michel-Beyerle, M.-E., Ed.) pp 333−339, Springer-Verlag, Berlin.

Blankenship, R. E., & Parson, W. W. (1979) *Biochim. Biophys. Acta 545*, 429−444.

Burghaus, O., Plato, M., Rohrer, M., Möbius, K., MacMillan, F., & Lubitz, W. (1993) *J. Phys. Chem. 97*, 7639−7647.

Chang, C.-H., El-Kabbani, O., Tiede, D., Norris, J., & Schiffer, M. (1991) *Biochemistry 30*, 5352−5360.

Crespi, H. L. (1982) *Methods Enzymol. 88*, 3−5.

Debus, R. J., Feher, G., & Okamura, M. Y. (1985) *Biochemistry 24*, 2488−2500.

Debus, R. J., Feher, G., & Okamura, M. Y. (1986) *Biochemistry 25*, 2276−2287.

El-Kabbani, O., Chang, C.-H., Tiede, D. M., Norris, J., & Schiffer, M. (1991) *Biochemistry 30*, 5361−5369.

Ermler, U., Fritzsch, G., Buchanan, S., & Michel, H. (1994) *Structure 2*, 925−936.

Feezel, L. L., Gast, P., Smith, U. H., & Thurnauer, M. C. (1989) *Biochim. Biophys. Acta 974*, 149−155.

Feezel, L. L., Reiss-Husson, F., Agalidis, I., Smith, U. H., Thurnauer, M. C., & Norris, J. R. (1990) *Appl. Magn. Reson. 1*, 255−265.

Feher, G. (1971) *Photochem. Photobiol. 14*, 373−387.

Feher, G., & Okamura, M. Y. (1978) in *The Photosynthetic Bacteria* (Clayton, R. K., & Sistrom, W. R., Eds.) pp 349−386, Plenum Press, New York.

Feher, G., & Okamura, M. Y. (1984) in *Advances in Photosynthesis Research* (Sybesma, C., Ed.) Vol. II, pp 155−164, Martinus Nijhoff/Dr. W. W. Junk, The Hague.

Feher, G., Okamura, M. Y., & McElroy, J. D. (1972) *Biochim. Biophys. Acta 267*, 222−226.
Franzen, S., Goldstein, R. F., & Boxer, S. G. (1990) *J. Phys. Chem. 94*, 5135−5149.
Füchsle, G., Bittl, R., van der Est, A., Lubitz, W., & Stehlik, D. (1993) *Biochim. Biophys. Acta 1142*, 23−35.
Gast, P., & Hoff, A. J. (1979) *Biochim. Biophys. Acta 548*, 520−535.
Gast, P., Hemelrijk, P. W., & Hoff, A. J. (1994) *FEBS Lett. 337*, 39−42.
Gast, P., Hemelrijk, P. W., Van Gorkom, H. J., & Hoff, A. J. (1996) *Eur. J. Biochem. 239*, 805−809.
Greenfield, S. R., Seibert, M., Govindjee, & Wasielewski, M. R. (1996) *Chem. Phys. 210*, 279−295.
Hale, M. B., Blankenship, R. E., & Fuller, R. C. (1983) *Biochim. Biophys. Acta 723*, 376−382.
Hoff, A. J., & Gast, P. (1979) *J. Phys. Chem. 83*, 3355−3358.
Hore, P. J. (1996) *Mol. Phys. 89*, 1195−1202.
Isaacson, R. A., Lendzian, F., Abresch, E. C., Lubitz, W., & Feher, G. (1995) *Biophys. J. 69*, 311−322.
Kirmaier, C., Holten, D., & Parson, W. W. (1985) *Biochim. Biophys. Acta 810*, 33−48.
Kirmaier, C., Holten, D., Debus, R. J., Feher, G., & Okamura, M. Y. (1986) *Proc. Natl. Acad. Sci. U.S.A. 83*, 6407−6411.
Klette, R., Törring, J. T., Plato, M., Möbius, K., Bönigk, B., & Lubitz, W. (1993) *J. Phys. Chem. 97*, 2015.
Kothe, G., Weber, S., Ohmes, E., Thurnauer, M. C., & Norris, J. R. (1994) *J. Am. Chem. Soc. 116*, 7729−7734.
Liu, B., van Kan, P. J. M., & Hoff, A. J. (1991) *FEBS Lett. 289*, 23−28.
Loach, P. A., & Hall, R. L. (1972) *Proc. Natl. Acad. Sci. U.S.A. 69*, 786−790.
Michel, H. (1991) in *Crystallization of Membrane Proteins*, p 211, CRC Press, Inc., Boca Raton.
Morris, A. L., Snyder, S. W., Zhang, Y., Tang, J., Thurnauer, M. C., Dutton, P. L., Robertson, D. E., & Gunner, M. R. (1995) *J. Phys. Chem. 99*, 3854−3866.
Müh, F., Rautter, J., & Lubitz, W. (1996) *Ber. Bunsen-Ges. Phys. Chem. 100*, 1974−1977.
Neugebauer, J. (1987) *A Guide to the Properties and Uses of Detergents in Biology and Biochemistry*, Calbiochem Brand Chemicals, La Jolla, CA.
Norris, J. R., Morris, A. L., Thurnauer, M. C., & Tang, J. (1990) *J. Chem. Phys. 92*, 4239−4249.
Prisner, T. F., van der Est, A., Bittl, R., Lubitz, W., Stehlik, D., & Möbius, K. (1995) *Chem. Phys. 194*, 361−370.
Proskuryakov, I. I., Klenina, I. B., Hore, P. J., Bosch, M. K., Gast, P., & Hoff, A. J. (1996) *Chem. Phys. Lett. 257*, 333−339.
Rautter, J., Lendzian, F., Lubitz, W., Wang, S., & Allen, J. P. (1994) *Biochemistry 33*, 12077−12084.
Rutherford, A. W., Agalidis, I., & Reiss-Husson, F. (1985) *FEBS Lett. 182*, 151−157.
Schelvis, J. P. M., Liu, B.-L., Aartsma, T. J., & Hoff, A. J. (1992) *Biochim. Biophys. Acta 1102*, 229−236.
Snyder, S. W., & Thurnauer, M. C. (1993) in *The Photosynthetic Reaction Center* (Norris, J. R., & Deisenhofer, J., Eds.) pp 285−330, Academic Press, New York.
Stehlik, D., Bock, C. H., & Thurnauer, M. C. (1989) in *Advanced EPR. Applications in Biology and Biochemistry* (Hoff, A. J., Ed.) Elsevier, Amsterdam.
Straley, S. C., Parson, W. W., Mauzerall, D. C., & Clayton, R. K. (1973) *Biochim. Biophys. Acta 305*, 597−609.
Tang, J., Bondeson, S., & Thurnauer, M. C. (1996) *Chem. Phys. Lett. 253*, 293−298.
Tiede, D. M., Vazquez, J., Cordova, J., & Marone, P. A. (1996) *Biochemistry 35*, 10763−10775.
Trifunac, A. D., Thurnauer, M. C., & Norris, J. R. (1978) *Chem. Phys. Lett. 57*, 471−473.
van den Brink, J. S., Hulsebosch, R. J., Gast, P., Hore, P. J., & Hoff, A. J. (1994) *Biochemistry 33*, 13668−13677.
van der Est, A., & Stehlik, D. (1996) in *The Reaction Center of Photosynthetic Bacteria* (Michel-Beyerle, M.-E., Ed.) pp 319−332, Springer-Verlag, Berlin.
van der Est, A., Bittl, R., Abresch, E. C., Lubitz, W., & Stehlik, D. (1993) *Chem. Phys. Lett. 212*, 561−568.
van der Est, A., Sieckmann, I., Lubitz, W., & Stehlik, D. (1995) *Chem. Phys. 194*, 349−359.
Wang, S., Lin, S., Lin, X., Woodbury, N. W., & Allen, J. P. (1994) *Photosynth. Res. 42*, 203−215.
Wraight, C. A. (1979) *Biochim. Biophys. Acta 548*, 309−327.
Wraight, C. A. (1982) in *Function of Quinones in Energy Conserving Systems* (Trumpower, B. L., Ed.) pp 181−197, Academic Press, New York.

BI9630319